

Supplementary Materials AND METHODS

Production and purification of GFP and IL-23 minicircle DNA and hydrodynamic delivery

Minicircle-RSV.Flag.mIL23.elasti.bpA or RSV.eGFP.bpA was produced as described (Chen et al., 2005). To produce minicircle-RSV.Flag.mIL23.elasti.bpA or RSV.eGFP.bpA, a single isolated colony from a fresh plate was grown for 8 hours in 2 ml of Luria–Bertani broth with kanamycin. Eight hundred microliters of this culture was used to inoculate 1 l of terrific broth and grown for an additional 17 hours. Overnight cultures were centrifuged at 20 °C, 4,000 r.p.m. for 20 minutes. The pellet was resuspended at 4:1 (v/v) in fresh Luria–Bertani broth containing 1% L-arabinose. The bacteria were incubated at 32 °C with constant shaking at 220 r.p.m. for 2 hours. After adding half volume of fresh low-salt Luria–Bertani broth (pH 8.0) containing 1% L-arabinose, the incubation temperature was increased to 37 °C, and the incubation was continued for an additional 2 hours. Episomal DNA minicircles (MC) were prepared from bacteria using EndoFree Megaprep plasmid purification kits from Qiagen (Chatsworth, CA) according to the manual instruction.

MC was prepared in lactated ringers solution and administered by hydrodynamic delivery into the tail vein. Mice were mechanically restrained and received a volume of 10% bodyweight containing 10- μ g MC within 5–7 seconds. Serum IL-23 was assayed using an ELISA kit purchased from Invitrogen (Carlsbad, CA) in accordance with the manufacturer's instructions.

Bile acid liquid chromatography with tandem mass spectrometry bioanalytical method

Cholic acid, α -muricholic acid, β -muricholic acid, chenodeoxycholic acid, deoxycholic acid, ursodeoxycholic acid, lithocholic acid, taurodeoxycholic acid, and tauroolithocholic acid were quantified by using the liquid chromatography with tandem mass spectrometry (LC-MS/MS) bioanalytical method as previously described (Alnouti et al., 2008). Briefly, 100 μ l of each calibrator and QC sample dissolved and diluted in methanol (MeOH, Thermo Fisher Scientific, Waltham, MA) were spiked with 20 μ l of 10 μ M D4-DCA in MeOH as the internal standard and blown dried and resuspended in 100 μ l of MeOH/H₂O = 50/50 (v/v) for LC-MS/MS injection. To analyze plasma samples, 100 μ l of the plasma was spiked with 20 μ l of 10- μ M D4-DCA in MeOH. One milliliter of the acetonitrile (ACN, Thermo Fisher Scientific) was then added to the mixture. After vortexing for 10 seconds and centrifuging for 5 minutes at 17,000g at room temperature, the resulting supernatant was moved to a fresh glass vial, blown dry, and resuspended in 100 μ l of MeOH/H₂O = 50/50 (v/v) for LC-MS/MS injection. To analyze other solid tissue samples, 200 μ l of H₂O was added to each of the frozen tissue samples (maintain about 50 mg of weight for each tissue sample) in a 2-ml grinding tube filled with 2.8-mm stainless steel grinding balls (SPEX SamplePrep, Metuchen, NJ). The vial was vigorously shaken in Geno and Grinder (2010) (SPEX SamplePrep, Metuchen, NJ) at 1,750 strokes/min at room temperature for 1 minute, repeated 3 times with 15 seconds of rest in-between. One hundred microliters of the resulting homogenates was transferred to a fresh microcentrifuge tube, spiked with 20 μ l of 10 μ M D4-DCA in

MeOH, and then mixed with 1 ml of ACN with 10 seconds of vortexing. After 5 minutes of centrifugation at 17,000g at room temperature, the resulting supernatant was moved to a fresh glass vial, blown dry, and resuspended in 100 μ l of MeOH/H₂O = 50/50 (v/v) for LC-MS/MS injection. Four microliters of each of the resuspended sample extracts mentioned above were injected into Waters (Milford, MA) Acquity I-Class FTN UPLC system and resolved with Waters Acquity UPLC BEH C18 Column (130 Å, 1.7 μ m, 2.1 mm \times 100 mm). The LC flow was continuously fed to Waters Xevo TQ-S triple quadrupole mass spectrometer for the bile acid (BA) identification and quantification. All LC-MS/MS settings can be found in the published paper (Alnouti et al., 2008). The lower limit of quantification for cholic acid, α -muricholic acid, β -muricholic acid, chenodeoxycholic acid, deoxycholic acid, ursodeoxycholic acid, lithocholic acid, taurodeoxycholic acid, and taurodeoxycholic acid are 0.01, 0.01, 0.01, 0.05, 0.01, 0.05, 0.05, 0.01, and 0.005 μ M, respectively.

Imiquimod-induced psoriasis model

Mice were treated daily for 5 days on each ear with 5 mg of 5% imiquimod cream (Taro Pharmaceuticals, New York, NY), or with control vehicle cream (Vanicream; Pharmaceutical Specialties, Cleveland, GA).

Histopathological analysis and immunohistochemistry

Formaldehyde-fixed, paraffin-embedded ear skin samples were stained with hematoxylin and eosin using standard procedures. The paw tissue was decalcified with 4% formic acid before embedding. Images were acquired using a Nikon Optiphot 2 microscope (Nikon, Tokyo, Japan). Epidermal thickness was measured with a computer-assisted quantitative image analysis software (ImageJ, National Institutes of Health, Bethesda, MD).

For immunohistochemical analysis, skin sections were incubated with primary antibodies against murine Ki-67 or phosphorylated STAT3, followed by the appropriate secondary antibodies. Rinsed sections were counterstained with hematoxylin.

In vitro BA treatment

For in vitro culture to test BA treatment, we planted 24-well plates with lymph node single-cell suspension (10⁶/ml) or ear skin fragments (~1/5 ear per well of scissor-cut, 1 mm in diameter small pieces) with RPMI 1640 culture medium supplemented with 10% fetal bovine serum. Once cells or tissues were planted, stimulating reagents, such as IL-23, IL-17A, or TNF- α , were added followed by BAs or BA agonists with an indicated concentration. Supernatant, cells, or tissue fragments were collected after 4 to 24 hours of incubation for further ELISA and RT-PCR examination.

Human samples

Elutriated lymphocytes were obtained from healthy donors by the Department of Transfusion Medicine, National Institutes of Health, under an Institutional Review Board–approved protocol (99-CC-0168). Written informed consent has been obtained from all healthy donors.

Transfection of CCR6+ Jurkat cells

Jurkat cells were stably transfected with a pORF-hCCR6 plasmid (InvivoGen, San Diego, CA) using Lipofectamine

2000 protocol and reagents from ThermoFisher Scientific. The efficiency of transfection was confirmed by flow cytometry.

Keratinocyte culture

HaCaT are established cell lines from ATCC (Manassas, VA). HaCaT cells were cultured in DMEM (Invitrogen) with 10% fetal bovine serum. For primary keratinocytes, adult mouse keratinocytes were cultured following the procedure described by Li et al. (2017). Briefly, the tail skin from an adult mouse was digested in dispase digestion buffer, which contains 4 mg/ml dispase II in supplemented KC growth medium (KC basal medium with 0.06 mM calcium chloride, Defined Growth Supplement, antibiotics) overnight at 4 °C. Epidermal sheet was removed, digested in a trypsin-based digestion solution. Then cells were filtered and seeded in supplemented KC growth medium in culture dishes pre-coated with a collagen-based coating material.

Quantitative real-time PCR

Total RNA of mouse ear skin was extracted using an RNeasy Fibrous Tissue Kit (Qiagen, Hilden, Germany). For paw tissue, the skin was removed from the hind paw before further extraction. Quantitative real-time PCR was performed using Quant Studio 3 real-time PCR system (Applied Biosystems, Foster City, CA). The primers were obtained from Integrated DNA Technologies (Skokie, IL). The primers listed in [Supplementary Table S2](#) were pre-designed (otherwise the sequence is shown) and obtained from Integrated DNA Technologies (Skokie, IL).

For human samples, cells were activated with eBioscience™ Cell Stimulation Cocktail (Thermo Fisher Scientific) for 3 hours and total cellular RNA was purified using the RNeasy Mini kit (Qiagen). Real-time PCR was performed using the SuperScript One Step RT-PCR kit (Life Technologies, Carlsbad, CA). Primer and probe sets (FAM/MGB-labeled) were purchased from Applied Biosystems (Waltham, MA). Results were normalized based on the values for GAPDH mRNA, detected using TaqMan GAPDH Control reagents (Applied Biosystems). To calculate the relative expression of a particular gene, the Δ CT was calculated from the CT values of the gene of interest minus CT value of GAPDH for each replicate of the duplicate values for each sample, and then the $2^{-\Delta$ CT was calculated and the biggest value of the duplicate was set at 100 to eliminate any donor to donor variation in actual expression. The rest of the lithocholic acid-treated samples were then calculated similarly to get their expression relative to control which was set at 100.

Flow cytometry and flow sorting

Anti-mouse $\gamma\delta$ -TCR (clone GL3), CD45 (30-F11), CD3(17A2), CCR6 (29-2L17), CD11b (M1/70), Ly6G (IA8) antibodies (BioLegend, San Diego, CA), anti-IL-17A (eBio17B7, eBioscience, San Diego, CA) were used for flow cytometry. Whole ear skin was minced and digested with Liberase TM (Roche, Mannheim) and Dnase I (Sigma-Aldrich, St. Louis, MO) with the addition of 5% fetal bovine serum to obtain whole skin cell suspensions before passing tissue through a 70- μ m cell strainer. Single-cell suspension from the cervical draining or popliteal lymph nodes was prepared by

mashing the tissue through a 70- μ m cell strainer. Intracellular staining was done after incubating cells for 2 hours with a cell stimulation cocktail (eBioscience). Anti-mouse CD16/32 (BD Biosciences, San Jose, CA) was added to cells before staining to block binding to Fc-receptors.

Anti-mouse CD31 (clone 390), CD45 (30-F11), CD11b (M1/70) antibodies (BioLegend) were used for flow sorting. The whole murine ear skin was incubated in PBS containing 0.5% trypsin (Sigma-Aldrich) for 30 minutes at 37 °C, and the epidermis was retrieved. Murine epidermis and whole skin were minced and digested separately. Flow sorting was done using the BD Influx Cell Sorter with 7-AAD (BioLegend) as the cell viability marker. CD45⁻/CD31⁺ endothelial and CD45⁺/CD11b⁺ myeloid cells were isolated from the whole skin, and CD45⁻ keratinocytes were isolated from the epidermis. Compensation was performed using Anti-Rat Ig, κ /Negative Control Compensation Particles Set (BD Biosciences).

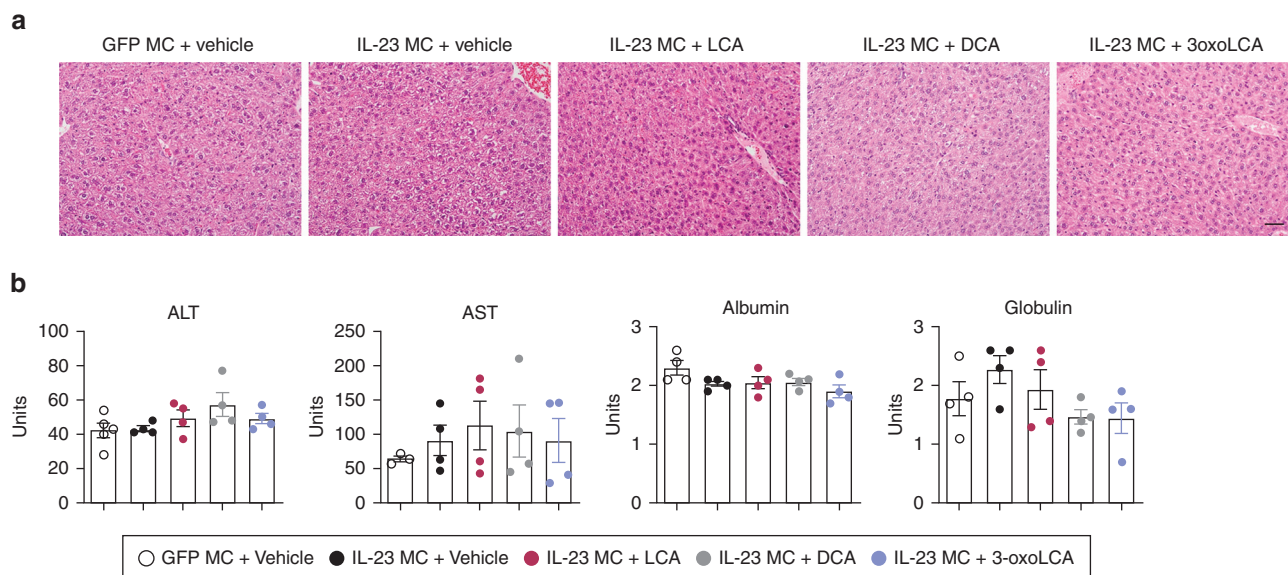
For purification of lymphocyte subsets from humans, CD4⁺ T cells were isolated from peripheral blood mononuclear cells by negative selection using RosetteSep CD4⁺ T cell enrichment cocktail (StemCell Technologies, Vancouver, Canada). Cells were stained with anti-CD4, anti-CD45RO, anti-CD127, anti-CD25, anti-HLA-DR, and anti-CCR6 (from eBioscience). All cell sorting was done using a FACS Aria flow cytometer (BD Biosciences). By post-sort analysis, the purity of populations was 95–99%. Cells were stimulated with Leukocyte Activation Cocktail, with GolgiPlus™ (BD Pharmingen, Franklin Lakes, NJ) for 6 hours at 37 °C before being stained with anti-IL-17A or anti-IFNG (eBioscience) by using Cytofix/CytoPerm Plus kit (BD Pharmingen). Cells were analyzed using an LSR II System flow cytometer (BD Biosciences), and the data were subsequently analyzed and presented using FlowJo software (TreeStar, Ashland, OR).

Chemotaxis assay

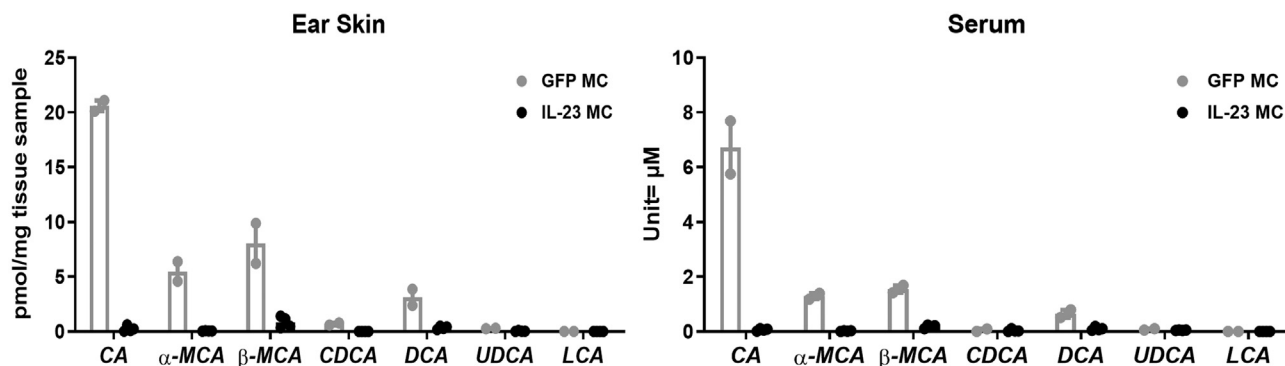
To evaluate the chemotactic ability of Jurkat T (with and without CCR6 overexpression) cells to the HaCaT keratinocyte conditioned medium, transwell migration assay was performed with ChemoTx system (Neuro Probe, Gaithersburg, MD). A-96 well chamber assembly with 5 μ m pore size was chosen according to Jurkat cell diameter. The supernatant was collected from cultured HaCaT cells and cell/debris was removed by centrifuge. A total of 30 μ l of supernatant were loaded in the bottom well, and 25 μ l of Jurkat or CCR6+ Jurkat cells were loaded above the membrane. The plates were covered and put in a cell incubator for 3 hours before collecting cells from bottom wells for counting by flow cytometry. The cell number in the bottom wells indicates the chemotactic ability of the lower medium to the upper cells.

SUPPLEMENTARY REFERENCES

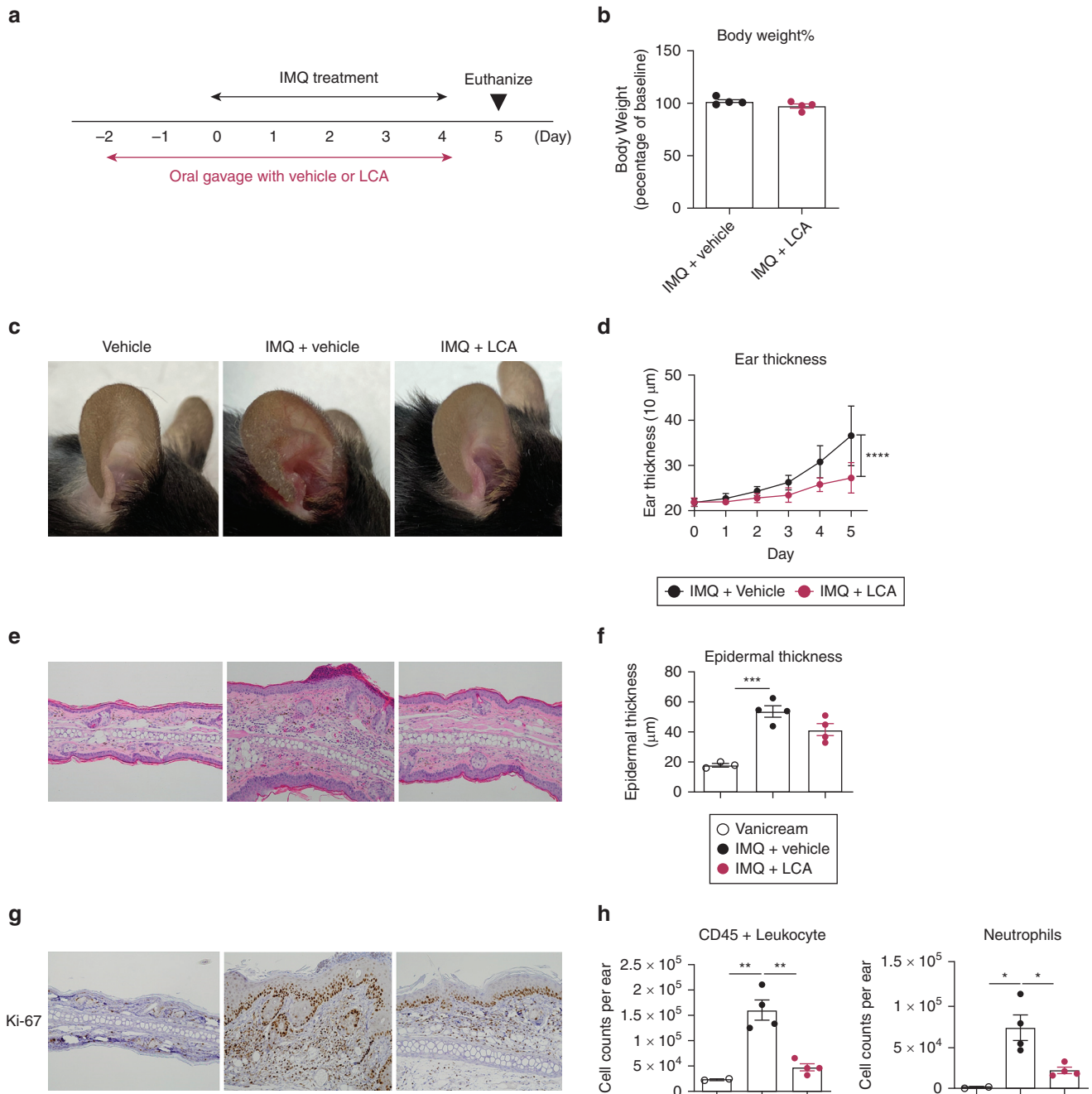
- Alnouti Y, Csanaky IL, Klaassen CD. Quantitative-profiling of bile acids and their conjugates in mouse liver, bile, plasma, and urine using LC-MS/MS. *J Chromatogr B Analyt Technol Biomed Life Sci* 2008;873:209–17.
- Chen ZY, He CY, Kay MA. Improved production and purification of minicircle DNA vector free of plasmid bacterial sequences and capable of persistent transgene expression in vivo. *Hum Gene Ther* 2005;16:126–31.
- Li M, Cai SY, Boyer JL. Mechanisms of bile acid mediated inflammation in the liver. *Mol Aspects Med* 2017;56:45–53.



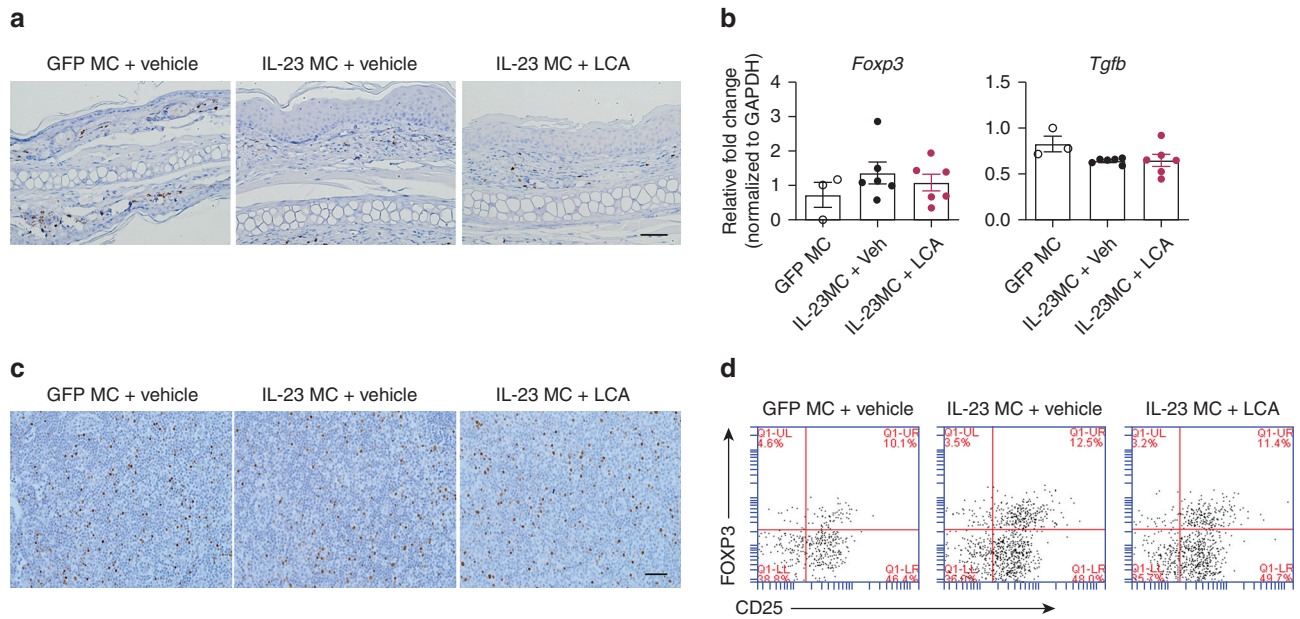
Supplementary Figure S1. No apparent hepatotoxicity induced by BAs. (a) Representative image of H&E-stained liver sections (Bar = 50 μ m) and (b) Serum levels of ALT, AST, albumin, and globulin from mice with indicated treatment. Data are presented as mean \pm SEM (n = 4). Data are representative of two independent experiments. ALT, alanine aminotransferase; AST, aspartate aminotransferase; BA, bile acid; LCA, lithocholic acid; MC, minicircle DNA.



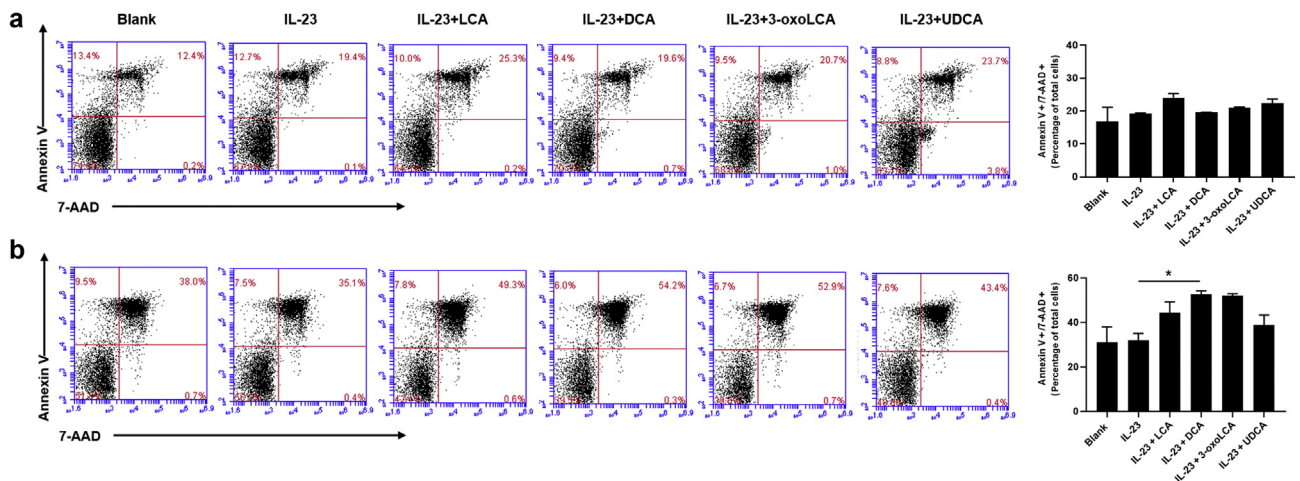
Supplementary Figure S2. Profile of BAs in ear skin and serum from mice at day 14 after delivery of GFP control MC or IL-23 MC. α -MCA, α -muricholic acid; β -MCA, β -muricholic acid; CA, cholic acid; CDCA, chenodeoxycholic acid; DCA, deoxycholic acid; LCA, lithocholic acid; MC, minicircle DNA; TDCA, taurodeoxycholic acid; TLCA, tauroolithocholic acid; UDCA, ursodeoxycholic acid.



Supplementary Figure S3. Oral administration of LCA ameliorates IMQ-induced PsD. (a) Schematic illustration of experimental protocols. Mice were orally administered PBS vehicle or LCA at a dose of 30 mg/kg/per day for 7 consecutive days, starting 2 days before IMQ application. (b) Percentage of body weight, (c) representative photographs, (d) time course of ear thickness, (e) image of H&E section (Bar = 50 μ m), (f) histological analysis of epidermal thickness, (g) representative images of immunohistochemical Ki-67 (Bar = 50 μ m) and (h) absolute numbers of CD45⁺ leukocytes and neutrophils in the ear skin. Data are presented as mean \pm SEM (n = 4). Data are representative of two independent experiments. **P* < 0.05, ***P* < 0.01. ****P* < 0.001. H&E, hematoxylin and eosin; IMQ, imiquimod; LCA, lithocholic acid; PsD, psoriasiform dermatitis.

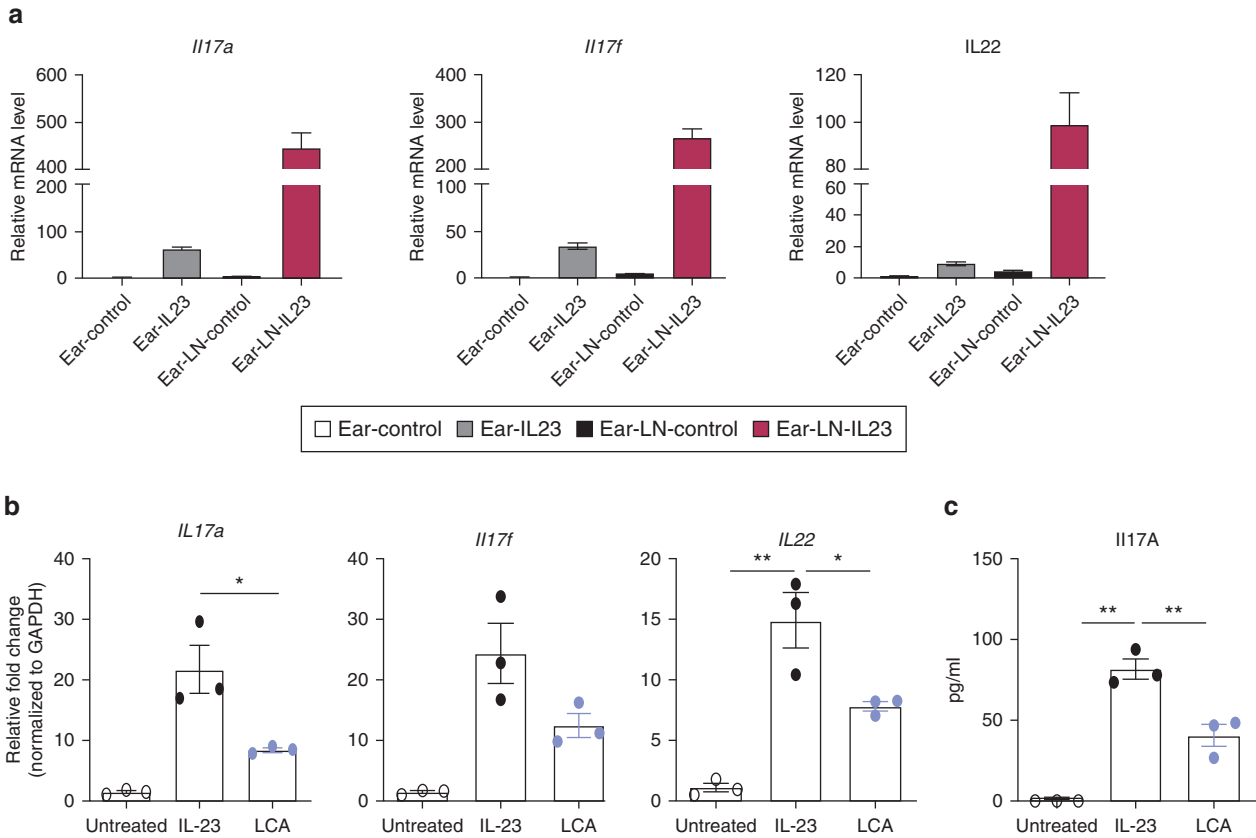
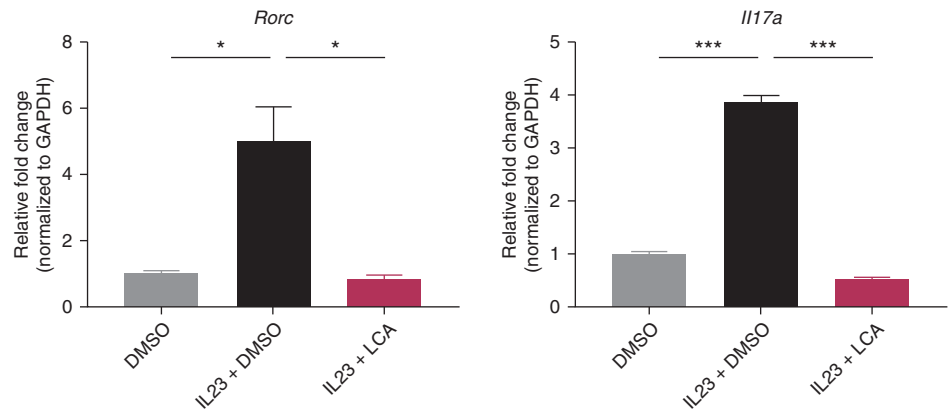


Supplementary Figure S4. LCA fails to affect the accumulation of Tregs in ear skin and draining lymph nodes from IL-23 MC-induced PsD. (a) Representative immunohistochemical images of Foxp3 in ear skin, (b) transcripts of Foxp3 and Tgfb in ear skin, (c) representative immunohistochemical images of Foxp3, and (d) representative flow cytometry plots showing the percentage of CD25⁺Foxp3⁺ Tregs (CD4⁺ gate) in the cervical lymph nodes from mice with treatment in Figure 2. Bar = 50 μ m. Data are presented as mean \pm SEM. * $P < 0.05$, ** $P < 0.01$, *** $P < 0.001$. LCA, lithocholic acid; MC, minicircle DNA; PsD, psoriasiform dermatitis.

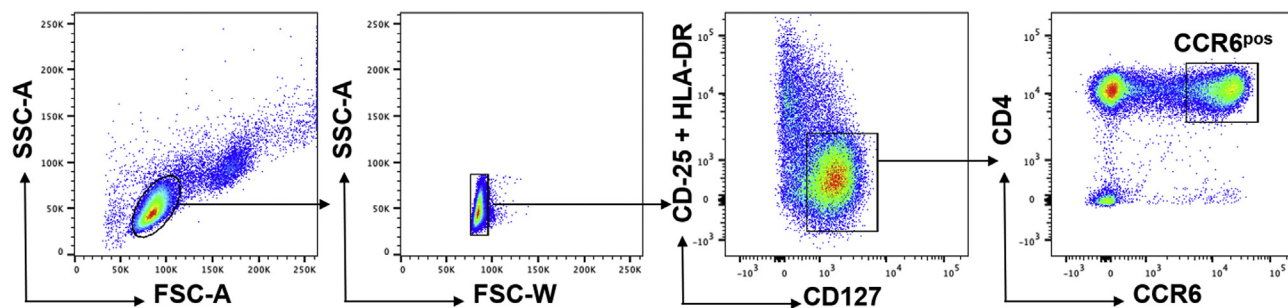


Supplementary Figure S5. Apoptotic rate of cLN cells induced by BAs. Single-cell suspension from cLN was cultured in the presence of IL-23 (100 ng/ml) with indicated BAs (50 μ M). Apoptosis was analyzed by flow cytometry at 4 hours (a) and 24 hours (b). Data are presented as mean \pm SEM. * $P < 0.05$. BA, bile acid; cLN, cervical lymph node; DCA, deoxycholic acid; LCA, lithocholic acid; UDCA, ursodeoxycholic acid.

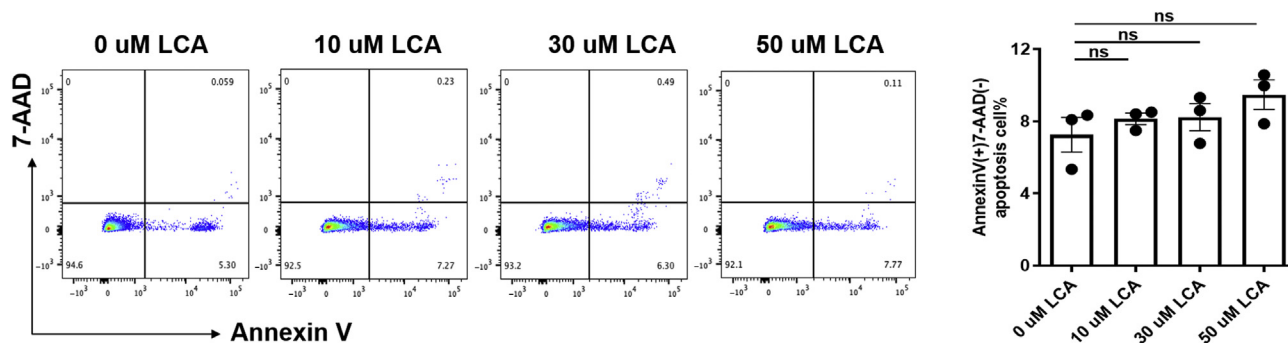
Supplementary Figure S6. Transcripts of *Rorc* and *Il17a* in cLN cells from naive mice, after 24 hours incubation in the presence of IL-23 (100 ng/ml) with LCA (50 μ M). cLN, cervical lymph node; LCA, lithocholic acid.



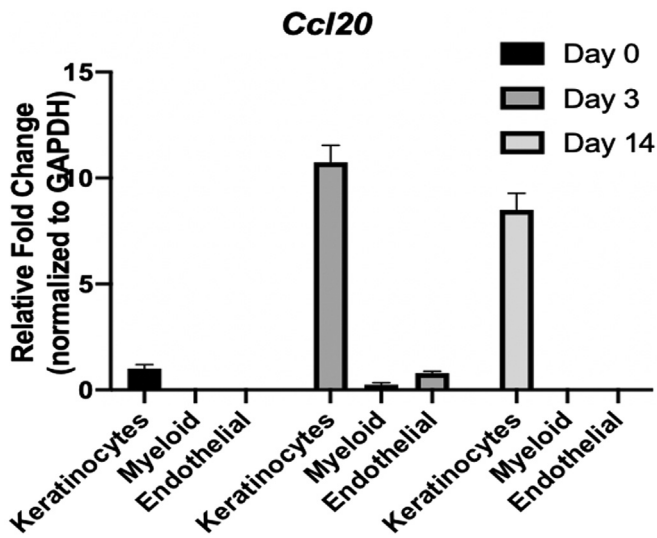
Supplementary Figure S7. LCA inhibits IL-17A production in a skin-LNs–derived coculture assay. Ear skin fragments from naive wild-type mice were cultured alone or with a single-cell suspension of cLNs from the same mice, in the presence or absence of IL-23 (100 ng/ml) for 24 hours. **(a)** Transcripts of Th17-related cytokines in tissue from above assay (n = 3). **(b)** Transcripts of Th17-related cytokines and **(c)** protein levels of IL-17A in the supernatants from skin-LNs coculture assay, followed by stimulation with IL-23 (100 ng/ml) for 24 hours. Data are presented as mean \pm SEM. Data are representative of two independent experiments. * P < 0.05, ** P < 0.01. *** P < 0.001. LCA, lithocholic acid; cLN, cervical lymph node; Th, T helper.



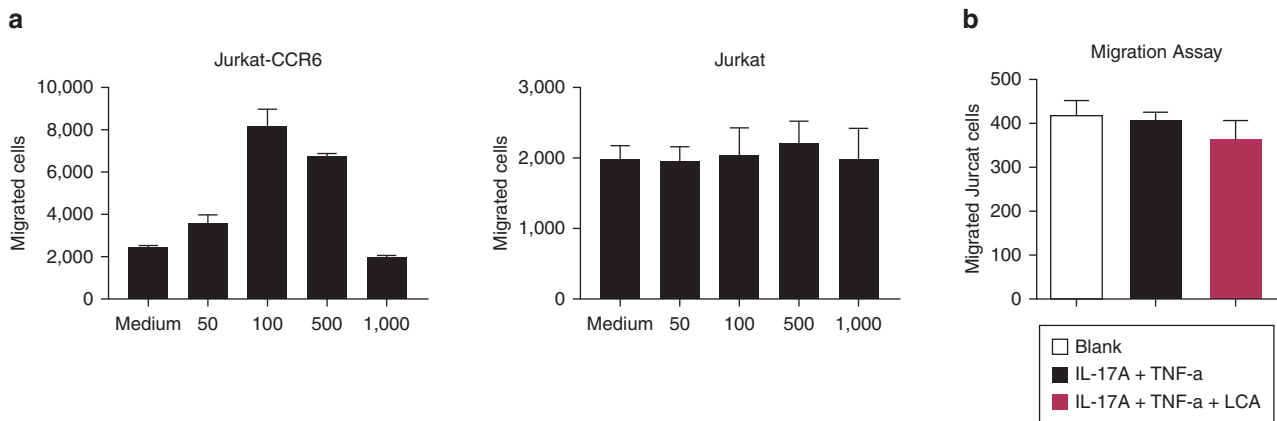
Supplementary Figure S8. Flow plots showing gating strategy for cell sorting of CCR6 positive cells from adult human blood. FSC, forward scatter; SSC, side scatter.



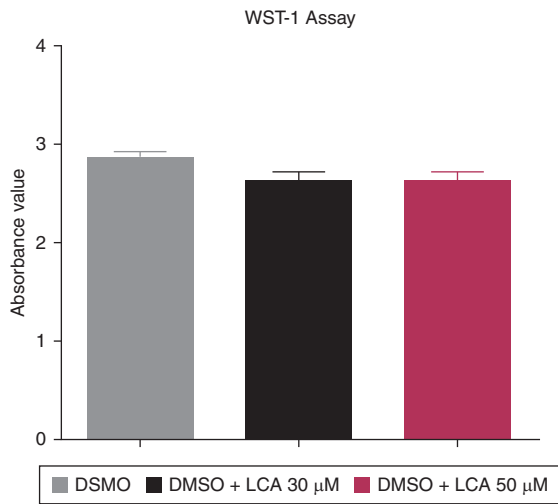
Supplementary Figure S9. Apoptotic rate of human $CD4^+CCR6^+$ T cells induced by LCA. Human $CD4^+CCR6^+$ T cells were cultured in the presence of LCA at the indicated concentration. Apoptosis was analyzed by flow cytometry at 16 hours. Data are presented as mean \pm SEM. LCA, lithocholic acid; ns, not significant.



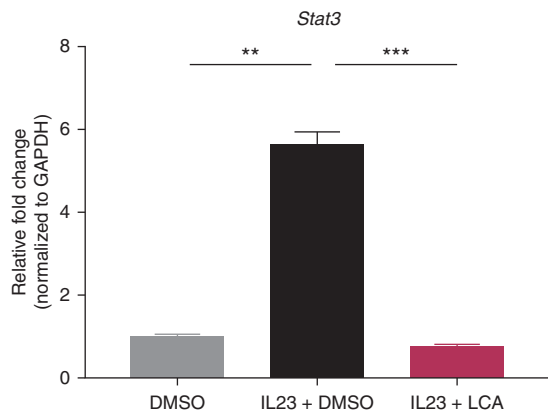
Supplementary Figure S10. CCL20 expression tends to predominantly originate from keratinocytes after injection of IL-23 MC. Keratinocytes, myeloid, and endothelial cells from the ear and dorsal skin were isolated from 4–5 mice using FACS on days 0, 3, and 14. CCL20 gene expression from these cell populations was identified. All data are presented as mean ± SEM. MC, minicircle DNA.



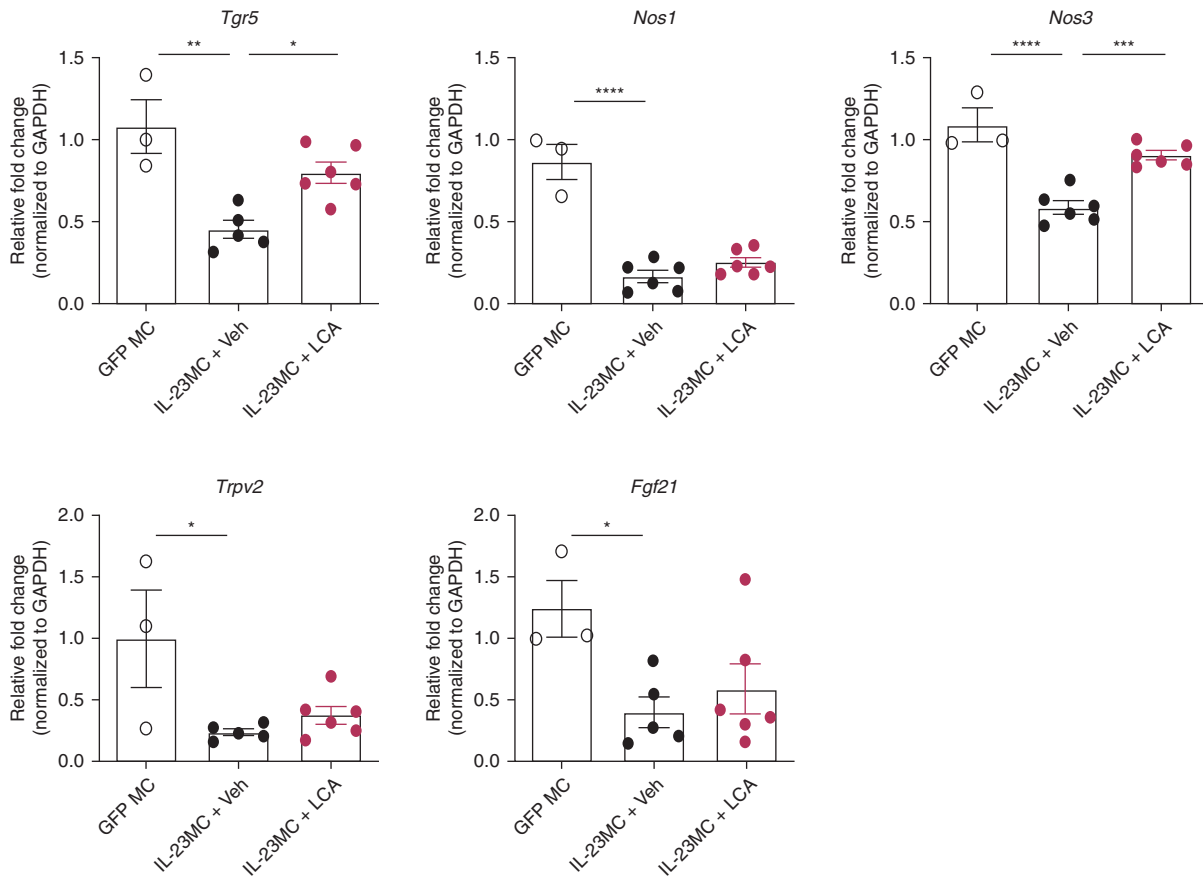
Supplementary Figure S11. Chemotaxis of CCR6 ± Jurkat cells is dependent on CCL20. (a) Migration of CCR6-overexpressing (CCR6+) Jurkat cells or normal Jurkat cells toward CCL20 at each indicated concentration (ng/ml). (b) Migration of Jurkat cells toward medium cultured with stimulated keratinocytes with or without LCA. Data are presented as mean ± SEM. LCA, lithocholic acid.



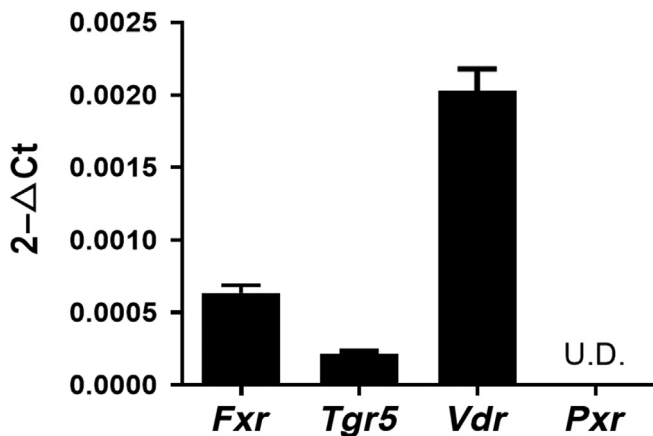
Supplementary Figure S12. LCA does not affect the viability of keratinocytes. The viability of keratinocytes was assessed by the water-soluble tetrazolium salt (WST-1) assay after coculturing with LCA (30 μ M or 50 μ M) for 16 hours. LCA, lithocholic acid.



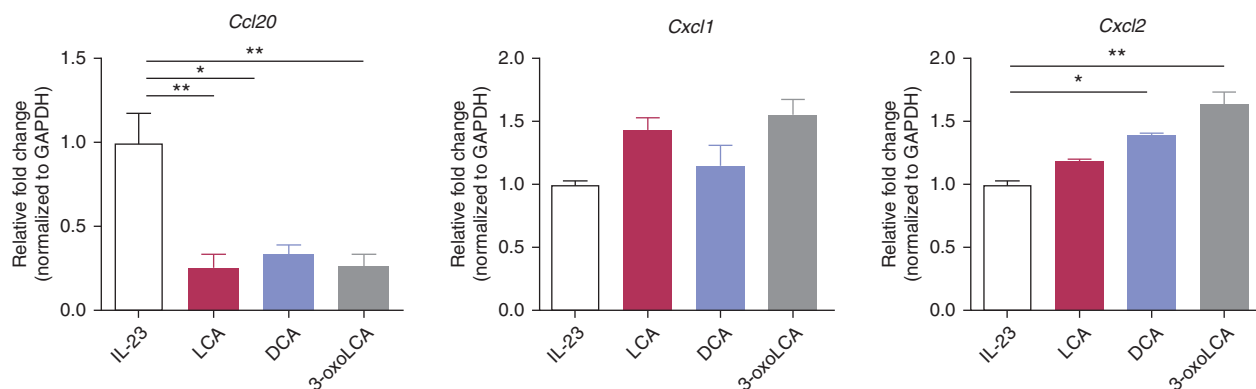
Supplementary Figure S13. Transcripts of *Stat3* in cLN cells, after 24 hours incubation in the presence of IL-23 (100 ng/ml) with LCA (50 μ M). cLN, cervical lymph node; LCA, lithocholic acid.



Supplementary Figure S14. *TGR5*-regulated signaling in the skin from IL-23 MC mice treated with vehicle or LCA. Transcripts of *TGR5*-regulated signaling genes in ear skin from mice delivered GFP MC, IL-23 MC + vehicle or IL-23 MC + LCA. Data are presented as mean ± SEM. * $P < 0.05$, ** $P < 0.01$. *** $P < 0.001$. LCA, lithocholic acid; MC, minicircle DNA; Veh, vehicle.



Supplementary Figure S15. mRNA levels of *Fxr*, *Tgr5*, *Vdr*, and *Pxr* in cervical lymph nodes from naive mice. Data are presented as mean ± SEM. U.D., undetectable.



Supplementary Figure S16. BAs inhibit CCL20 production in a skin-LNs-derived coculture assay. Ear skin fragments from naive wide-type mice were cultured alone or with a single-cell suspension of cLNs from the same mice in the presence or absence of IL-23 (100 ng/ml) for 24 hours. Transcripts of *Ccl20*, *Cxcl1*, and *Cxcl2* in the tissue from the above assay ($n = 2-3$). Data are presented as mean \pm SEM. * $P < 0.05$, ** $P < 0.01$, *** $P < 0.001$. BA, bile acid; cLN, cervical lymph node; DCA, deoxycholic acid; LCA, lithocholic acid.

Supplementary Table S1. Profile of BAs in Ear Skin and Serum from Mice at Day 14 after Delivery of GFP Control MC or IL-23 MC

| Sample# | Group | CA | alpha-MCA | beta-MCA | CDCA | DCA | UDCA | LCA | TDCA | TLCA |
|----------|------------|----------|-----------|----------|----------|----------|----------|--------|----------|----------|
| Plasma | GFP MC-1 | 21.103 | 6.3906 | 9.8859 | 0.602 | 3.8682 | 0.2652 | 0.0062 | ND | ND |
| Plasma | GFP MC-2 | 20.1136 | 4.5964 | 6.2244 | 0.7858 | 2.3766 | 0.3032 | <LLOQ | ND | ND |
| Plasma | IL-23 MC-1 | 0.6141 | 0.0724 | 1.4074 | ND | 0.4175 | 0.0906 | ND | ND | ND |
| Plasma | IL-23 MC-2 | 0.0357 | 0.0325 | 0.3393 | 0.0107 | 0.1828 | 0.0382 | <LLOQ | ND | ND |
| Plasma | IL-23 MC-3 | 0.1028 | 0.0511 | 1.153 | ND | 0.4854 | 0.008 | ND | ND | 0.0007 |
| Plasma | IL-23 MC-4 | 0.2335 | 0.0601 | 0.4689 | ND | 0.29 | 0.0323 | <LLOQ | 0.0342 | ND |
| Sample# | Group | CA | alpha-MCA | beta-MCA | CDCA | DCA | UDCA | LCA | TDCA | TLCA |
| Ear skin | GFP MC-1 | 5.754394 | 1.181239 | 1.417064 | ND | 0.799261 | 0.053661 | ND | 0.936942 | 0.040245 |
| Ear skin | GFP MC-2 | 7.68547 | 1.396588 | 1.691015 | 0.0932 | 0.511894 | 0.105909 | <LLOQ | ND | ND |
| Ear skin | IL-23 MC-1 | 0.084021 | 0.027536 | 0.216055 | 0.020476 | 0.101673 | 0.052955 | <LLOQ | ND | ND |
| Ear skin | IL-23 MC-2 | 0.012003 | ND | 0.107321 | ND | 0.049424 | 0.051542 | ND | ND | ND |
| Ear skin | IL-23 MC-3 | 0.052248 | 0.013415 | 0.237942 | 0.106615 | 0.1864 | 0.033891 | ND | ND | ND |
| Ear skin | IL-23 MC-4 | 0.103085 | 0.031773 | 0.174397 | 0.021888 | 0.072724 | 0.036009 | <LLOQ | ND | ND |

Abbreviations: alpha-MCA, alpha-muricholic acid; beta-MCA, beta-muricholic acid; CA, cholic acid; CDCA, chenodeoxycholic acid; DCA, deoxycholic acid; LCA, lithocholic acid; LLOQ, lower limit of quantification; MC, minicircle DNA; ND, not detected; TDCA, taurodeoxycholic acid; TLCA, tauroolithocholic acid; UDCA, ursodeoxycholic acid.

S/N<3

Unit = μ M or pmol/mg tissue sample.

Supplementary Table S2. Profile of BAs in ear skin and serum

| Gene Name | Identifier or Sequence |
|---------------|---|
| <i>Gapdh</i> | Mm.PT.39a.1 |
| <i>Il17a</i> | Mm.PT.58.6531092 |
| <i>Il17f</i> | Mm.PT.58.9739903 |
| <i>IL22</i> | F:5'-ATG AGT TTT TCC CTT ATG GGG AC-3', R: 5'-GCT GGA AGT TGG ACA CCT CAA-3' |
| <i>Rorc</i> | Mm. PT. 58.8455991 |
| <i>Tgr5</i> | Mm.PT.58.14275002.g |
| <i>Nos1</i> | Mm.PT.58.11089624 |
| <i>Nos3</i> | Mm.PT.58.12579546 |
| <i>Trapv2</i> | Mm.PT.58.9655908 |
| <i>Fgf21</i> | Mm. PT. 58.29365871.g |
| <i>CCL20</i> | Mm.PT.58.13906306 |

Ear skin and serum from mice at day af14 after delivery of GFP control MC or IL-23 MC were sampled and analyzed as described in [Materials and Methods](#).